

# Buckling Behaviour of LVL Beams

Prepared by:

B.F. Hutchings Timberbuilt Pty Ltd

J.Carson. CTE Consulting

27<sup>th</sup> June 2007

## Summary:

*Testing and analysis has been carried out to compare the observed effect of slenderness on the moment capacity of laminated veneer lumber beams with that predicted by the design procedures in AS 1720.1.*

*The results indicate that for slenderness ratios greater than 10, the design method in AS 1720.1 results in a significant underestimation of moment capacity. The underestimation can only be partly attributed to the measured weak axis bending rigidities and torsional rigidities significantly exceeding the nominal design values and considerable scope exists to refine design procedures for LVL beams to optimise material use.*

## Introduction

The design rules in AS 1720.1(Ref. 1) that predict the effect of slenderness on the load carrying capacity of LVL beams are the same as those applying for sawn, graded timber. LVL is however, significantly more uniform than sawn timber and is therefore straighter and much less variable in respect of its strength and stiffness. This uniformity is likely to make LVL less prone to slenderness related buckling and therefore allow efficient use of more slender sections enhancing competitiveness against non-wood based materials

## Objective:

To conduct a series of tests on LVL beams to observe their buckling behaviour and compare the behaviour with that predicted by the design rules of AS 1720.1.

## LVL Beams:

The LVL beams used in the tests were Product Certified by the Engineered Wood Products Association of Australasia (EWPAA) as having been manufactured and supplied to meet the requirements of AS/NZS 4357.0 (Ref. 2).

The LVL structural properties specified in the technical data sheets of the manufacturer are listed in Table1.

Bending strength	$f_b$	48 (MPa)
Modulus of elasticity – on edge	$E_x$	13,200 (MPa)
Modulus of elasticity – on flat	$E_y$	13,200 (MPa)
Modulus of rigidity	$G$	660 (MPa)

The nominal dimensions of the beams used in the tests were 300x42x5,600 mm (  $d \times b \times L$  ). The length  $L$  of the beams was chosen to enable the bending tests to be performed at the standardised span to depth ratio as specified in AS/NZS 4357.2 (Ref. 3), This Standard requires the test span to be 18 times the beam depth in a four point bending test, as illustrated in Figure 1.

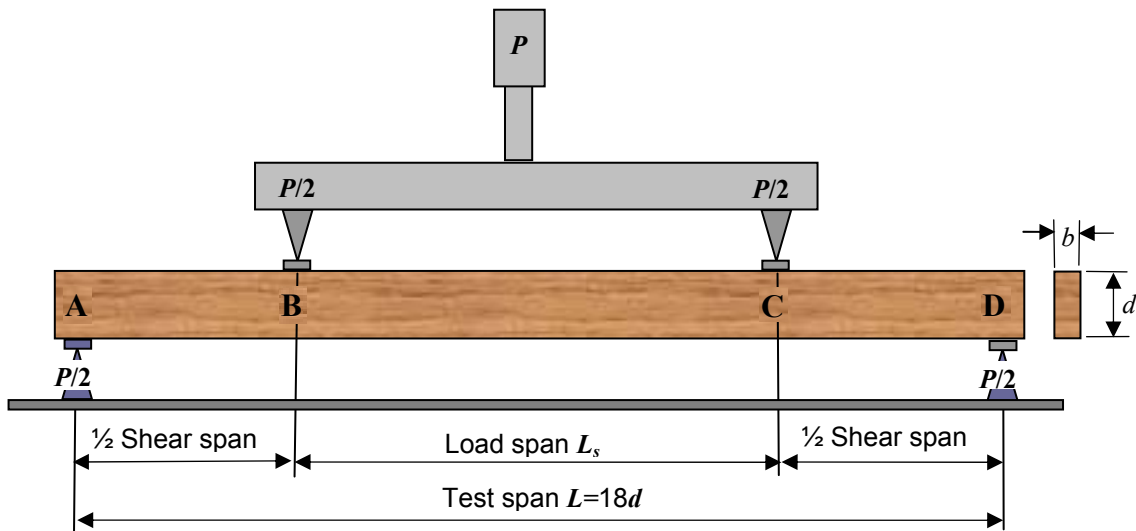


**Figure 1: Four point bending test configuration**

**Test laboratory:**

Tests were conducted at Melbourne Testing Services (MTS) under the supervision of the authors. MTS is a NATA accredited testing laboratory and has the necessary testing facilities and apparatus to conduct the bending and torsion tests.

The testing apparatus was appropriately instrumented to monitor, measure and record loading rates and displacements (vertical and lateral) necessary for determination of the following properties.

- a) Flexural rigidities  $EI_x$ , and  $EI_y$  about the  $x$ -axis and  $y$ -axis respectively;
- b) Torsional rigidity  $GJ$ ;
- c) Lateral buckling limit state moments; and
- d) Strength limit state moments.

The rigidity properties were required for the analysis in order to determine their influence on the lateral buckling limit state moment calculated using the design rules of AS 1720.1.

Photographs taken during the testing operations are provided in Appendix 1.

**Limit state moments:**

For this report the *lateral buckling and strength limit state moments* are for the purpose of interpreting the uniform bending moments imposed over the load span  $L_s$  during testing; these *limit state moments* are defined as follows.

*Lateral buckling limit state moment  $M_{LB}$ :*

This is a measure of the buckling capacity of a beam to resist the effects of uniform bending applied bending moments across the load span  $L_s$  as in Figure 1. The *lateral buckling limit state moment* is assumed to correspond to the peak applied load that can be resisted by the buckling capacity of a beam without failure. The buckling capacity of the beam is a function of flexural and torsional rigidities  $EI_y$  and  $GJ$

The peak applied load is observed by monitoring the point at which the applied loads begin to decrease relative to increases in the vertical and lateral displacements of a beam at mid-span. A beam will return to its pre-unloaded vertical state when the peak applied load is terminated.

*Strength limit state moment  $M_{SL}$ :*

This is a measure of the bending capacity of a stable beam to resist the effects of applied bending moments. A stable beam refers to a beam that is restrained from buckling under the action effects of the imposed bending moments. The bending capacity of a stable beam is a function of flexural strength and is determined by destructive testing in accordance with AS/NZS 4357.2. Therefore, the maximum *strength limit state moment* of a stable beam is assumed to correspond to the imposed bending moment at fracture.

**Load cases for edgewise bending tests:**

Three load cases 1, 2 and 3 with lateral restraint distances  $L_{ay}$  of 3,500 mm, 1,800mm and 900mm respectively were chosen for edgewise bending tests. The four point load configurations for these three load cases are illustrated in Figure 2.

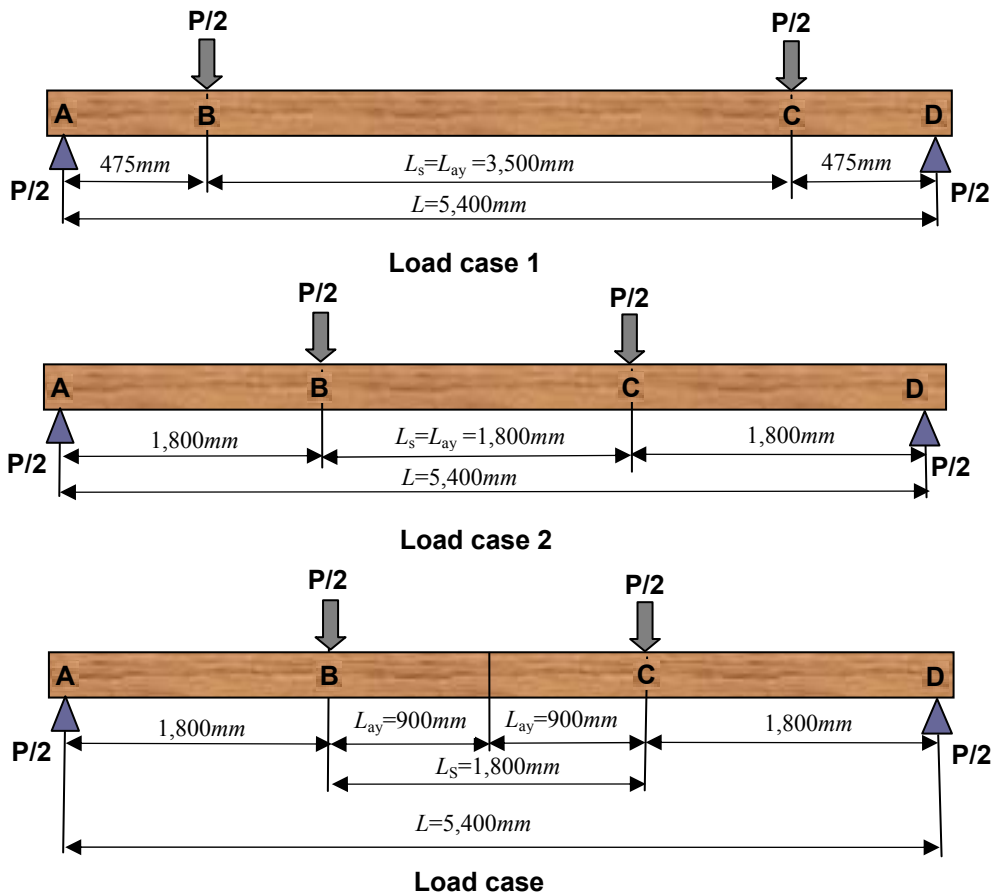


**Figure 2: Load cases for load spans  $L_S$  and lateral restraints  $L_{ay}$**

Lateral buckling and rotational restraints were positioned at the load points B and C for all three load cases illustrated in Figure 2. End restraints were not installed at load points A and D when the beams were tested with  $L_{ay} = 3,500\text{ mm}$  but were installed at these load points when the beams were tested for  $L_{ay} = 1,800\text{ mm}$  and  $900\text{ mm}$ . The loading configurations for load cases 2 and 3 correspond to AS/NZS 4357.2.

It was expected that for load case 1 and load case 2 the beams would reach their *lateral buckling limit states moments*  $M_{LB}$  without reaching their *strength limit states moments*  $M_{SL}$ .

For load case 3 the length of the load span  $L_S$  between load points  $B$  and  $C$  is the same as for load case 2, however, midway between these load points and additional lateral restraint was positioned at point  $E$  to reduce  $L_{ay}$  to 900 mm.

It was expected that for load case 3 that the mid-span restraint would prevent lateral buckling and, hence, the beams could be tested to destruction to determine their *strength limit states moment*  $M_{SL}$ .

For the three lateral restraint conditions illustrated in Figure 2, the uniform bending moment induced over the over the length of the load span is given by,

$$M = \frac{P(L - L_S)}{4}$$

### **Testing Procedures:**

The order in which testing and measurements proceeded are as follows.

1. Check of compliance with AS/NZS 4357.0
2. Edge-wise bending tests for load case 1.
3. Torsion tests.
4. Edgewise bending tests for load cases 2 and 3.
5. Flat-wise bending tests.

The same beams were used in the tests associated with 1, 2 ,3 and 4. Specimens for 5 were cut from the ends of tests beams from 4.

#### 1. Check of compliance with AS/NZS 4357.0

Prior to testing all beams were checked by EWPA representatives for conformance with the specification for manufacture prepared in accordance with AS/NZS 4357.0. The cross-sectional dimensions were measured and recorded for later analysis.

#### 2. Edge-wise bending tests for load case 1

Load and displacement data were continuously monitored and when the peak load was deemed to have been reached for each beam the loading was terminated.

All beams buckled without failure and returned to their vertical state once they were unloaded.

The load and displacement data were subsequently used in the analysis to determine the flexural rigidity  $(EI)_x$ , for each beam. The peak load was used to determine the *lateral buckling limit state moment* for each beam.

#### 3. Torsion tests.

The beams in the previous bending test were used in the torsion tests. The beams were restrained against rotation at mid-span and torsion applied through load applied to a lever arm fixed to end of the beams. Details can be observed in the photographs in Appendix 1. The load and displacement data during these torsion tests were subsequently used in the analysis to determine the torsional rigidity  $(GJ)$  of each beam.

#### 4. Edgewise bending tests for load cases 2 and 3.

The procedure to be followed was to initially test for load case 2 observe the peak loads, then unload the beams, fix a restraint to reduce  $L_{ay}$  to 900 mm and reload the beams to destruction as per load case 3.

The peak loads for load cases 2 were to be used in the analysis for determining the *lateral buckling limit states moments*. The failure load for load case 3 to be used in the analysis for determining *strength limit states moments*.

However, during testing for load case 2 half the beams failed without buckling, while the other half failed after the restraint was fixed to reduce  $L_{ay}$  to 900 mm as per load case 3. The failure mode of the beams in load case 2 was similar to that of a restrained beam, there was little or no lateral displacement as the beams moved through a vertical plane. For load case 2 it was difficult to judge by observing the monitors when a beam had reached its peak load and could therefore be terminated and the beam unloaded. This outcome was not expected. This is elaborated under Analysis and Results.

#### 5. Flat-wise bending tests

Test specimens were cut from the ends of the beams from the previous testing. The test span of the specimens was 18 times their breadth. Specimens were tested in four point loading with the loads applied at the third points. All specimens were tested to failure. The load displacement data from these test were used to the determine the flexural rigidity  $(EI)_y$  for each beam.

#### **Analysis and results:**

The statistical properties the data measured from the three load cases are summarised in Tables 2, and 3. Table 2 summarises flexural and torsional rigidities and Table 3 summarises moment capacities..

#### *Statistical procedures*

The procedures described in AS/NZS 4357.3 (Ref. 3) were applied for calculating the statistical properties listed in Table 2, 3 and 4.

#### *Statistical notation*

The following Legend for the statistical properties applies to all three tables

#### **Legend:**

$N$	Number specimens
$X_{\min}$	Minimum value
$X_{\max}$	Maximum value
$X_{\text{average}}$	Average (fiftieth) point estimate
$X_{\text{CoV}}$	Coefficient of variation
$X_{50,75}$	Fiftieth percentile estimated with 75% confidence level
$X_{05}$	Fifth percentile point estimate
$X_{05,75}$	Fifth percentile estimated with 75% confidence level

#### *Flexural rigidities and torsion rigidity.*

Table 2 summarises the statistical properties related to beam size, flexural and torsional rigidities.

**Table 2: Summary of flexural and torsional rigidities.**

Statistical Property	Size		Edgewise bending				Flatwise bending		Torsion	
			Load case 1		Load case 2					
	d	b	$E I_x$		$E I_x$		$E I_y$		$GJ$	
			Measured	Calculated	Measured	Calculated	Measured	Calculated	Measured	Calculated
mm	mm	Nmm <sup>2</sup>	Nmm <sup>2</sup>	Nmm <sup>2</sup>	Nmm <sup>2</sup>	Nmm <sup>2</sup>	Nmm <sup>2</sup>	Nmm <sup>2</sup>	Nmm <sup>2</sup>	
$N$	20	20	20	20	20	20	20	20	20	20
$X_{min}$	300.8	43.4	1.19E+12		1.22E+12		2.71E+10		7.31E+09	
$X_{max}$	301.4	44.7	1.43E+12		1.40E+12		3.50E+10		8.87E+09	
$X_{average}$	<b>301.1</b>	<b>44.1</b>	<b>1.35E+12</b>	<b>1.25E+12</b>	<b>1.33E+12</b>	<b>1.25E+12</b>	<b>3.16E+10</b>	<b>2.44E+10</b>	<b>8.14E+09</b>	<b>4.46E+09</b>
$X_{CoV}$	0.0	0.71%	3.88%		3.41%		6.50%		4.62%	
$X_{50,75}$	301.0	44.0	1.34E+12		1.33E+12		3.13E+10		8.08E+09	
$X_{05}$	300.8	43.6	1.27E+12	1.06E+12	1.26E+12	1.06E+12	2.83E+10	2.07E+10	7.52E+09	
$X_{05,75}$	300.7	43.5	1.25E+12		1.25E+12		2.77E+10		7.42E+09	

*Measured* means derived from the test data

*Calculated* means derived from the manufacturers published characteristic properties and nominal dimensions

In Table 2 the  $E I_x$  values derived for Load cases 1 and 2 are statistically the same, the difference of 1.5% between these values can be attributed shear effects. It can be observed from Table 2 that,

- $E I_x$  values derived from these tests are around 8% greater than the corresponding values calculated using the manufacturers published  $E_x$  design value (listed in Table 1) and the nominal dimensions; and .
- $E I_y$  values derived from these tests are around 29% greater than those calculated using the manufacturers published  $E_y$  and nominal dimensions.

The observed higher on-flat rigidity  $E I_y$  is likely to be a result of higher stiffness veneers being used for the outer plies of the LVL construction than those used for the core.

The  $GJ$  values measured for these test beams were found to be 58% greater than those calculated using the AS 1720 formula for estimation of  $J$  and the value for  $G$  published by the manufacturer and corresponding to the relationship,  $G = E/20$  given in AS 1720.1 for structural laminated veneer lumber. The significant difference between the observed torsional rigidity and that derived by calculation may be due to any of the following.

- The modulus of rigidity  $G$ , given in AS 1720.1 may only apply for calculating shear deflection of beams and may be conservative for calculation of torsional rigidity.
- The assumption that the resistance to twisting deformation of a rectangular section with an anisotropic material may not simply be reflected by the calculation of  $GJ$  where  $J$  is calculated using the expression given in AS 1720.

‘Load case 1’

For this load case two types of buckling modes were observed, these are illustrated in Figures 3 and 4.

In Figure 3 the beam’s lateral displacement was linear up to *critical elastic lateral buckling moment*  $M_{CR}$ , then commenced to buckle through a non linear lateral displacement before the loading was terminated. The loading was terminated when it was deemed that the  $M_{LB}$  had been reached by visual observation and observing the load-displacement readings on the recording monitor.

It can be observed from the data presented in Figure 3 that the ratio  $M_{LB}/M_{CR}=1.8$ ; this value is a function of  $L_{ay}$ . The relationships between  $\Delta_x$  and  $\Delta_y$  at the  $M_{CR}$  and  $M_{LB}$  points are also shown in Figure 3.

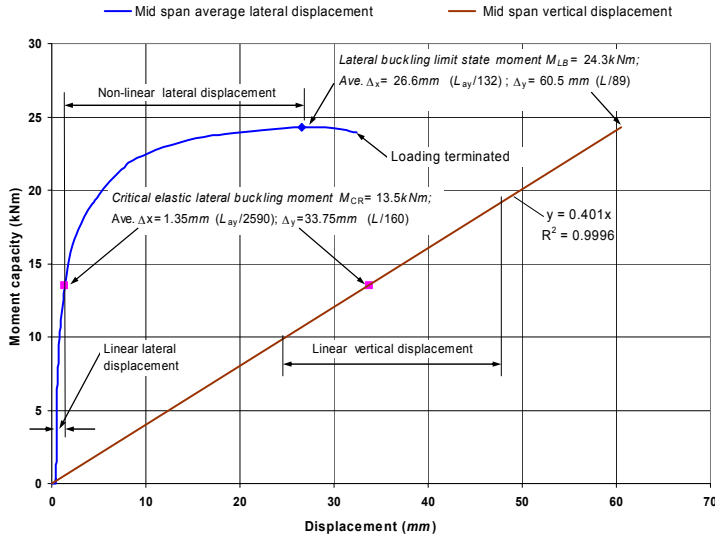


Figure 3: Moment capacity vs displacements for Load case 1 ( $L_{ay}=3,500mm$ )

By comparison to Figure 4, it can be observed in Figure 4 that the beam continued to be displaced vertically well beyond the  $M_{CR}$  before commencing to buckle laterally. The ratio  $M_{LB}/M_{CR}=1.7$  which is consistent with the ratios from Figure 3.

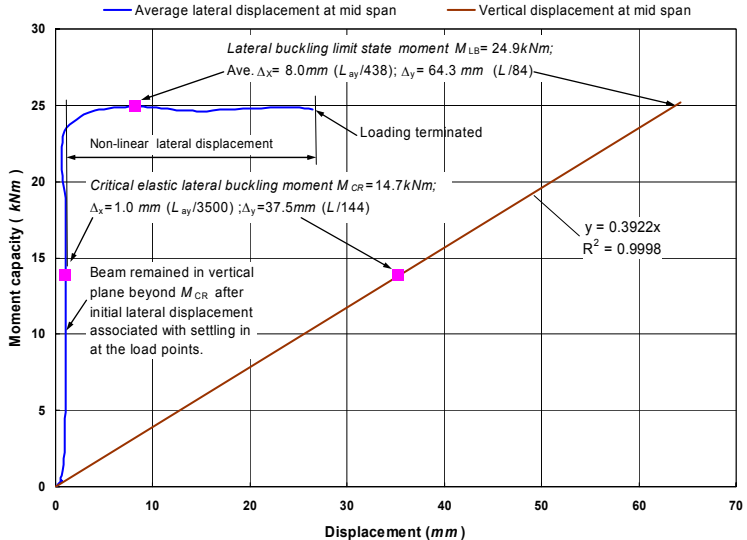


Figure 4: Moment capacity vs displacements for Load case 1 ( $L_{ay}=3,500mm$ )

The difficulty of judging, by visual observation and observing the load-displacement readings on the recording monitor, when the peak load corresponding to the lateral buckling limit state moment  $M_{LB}$  had been reached, can be observed in Figure 4 where the average lateral displacement  $\Delta_x$  continued nearly 20 mm beyond the peak load corresponding to  $M_{LB}$  before the loading was terminated.

It can be observed in Figures 3 and 4 that the regression equations of Moment capacity against  $\Delta_x$  are, statistically, strongly correlated as can be observed by the coefficient of

determination  $R^2$ ; this strong correlation is due to the very low coefficient of variation in  $EI_x$ , as listed in Table 2. All beams tested exhibited strong correlation between Moment capacity against  $\Delta_x$ .

‘Load cases 2 and 3’.

For Load case 2, two types of buckling modes were observed; these are illustrated in Figures 5 and 6.

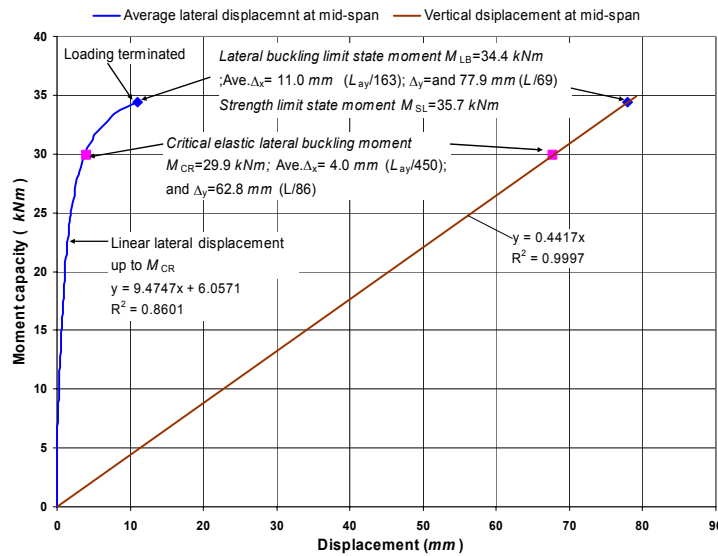


Figure 5: Moment capacity vs displacements for Load cases 2 and 3

The lateral displacement curve of  $\Delta_x$  in Figure 5 can be compared with the same curve in Figure 4. The difference between these curves can be readily observed. The problems experienced in judging the point at which the peak load causing lateral buckling occurred with Load case 2 for  $L_{ay}=1,800\text{ mm}$  has been as commented upon previously. It was expected that identifying the point at which *lateral buckling limit state moment*  $M_{LB}$  was reached would not present a problem for beams tested with an  $L_{ay}=1,800\text{ mm}$ .

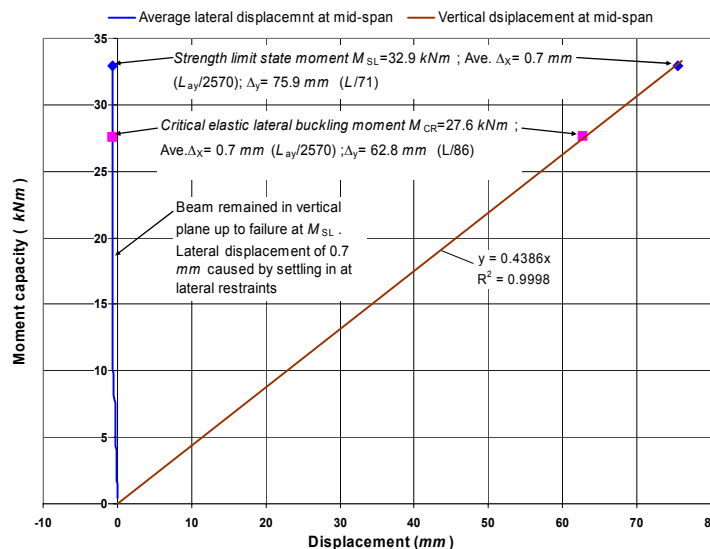


Figure 6: Moment capacity vs displacements for Load cases 2 & 3

Half the beams tested behaved in the manner similar to that illustrated in Figure 5, whereas, the other half fractured, before any visible buckling and lateral displacement readings could

be observed, these beams behaved in a manner similar to that illustrated in Figure 6, it was as though they were laterally restrained against buckling.

In Figure 5 the moment capacity corresponding the termination of the loading is at best indicative of  $M_{LB}$ . When the mid-span restraint was fitted for Load case 3, the average value of the *strength limit states moment*  $M_{SL}$  for these beams was just 4% above their average value for  $M_{LB}$ . In other words, those beams that did not fracture for Load case 2 for  $L_{ay}=1,800\text{ mm}$  were in fact very close to their  $M_{SL}$ ; this can be observed in Figure 6 where the ratio  $M_{SL}/M_{LB}=1.038$ . As a consequence of this outcome the strength data for those beams that fractured without a mid-span restraint and those that fractured with a mid-span restraint were merged to form one data set for analysis.

It can be observed in Figures 5 and 6 that the ratio  $M_{LB}/M_{CR} = 1.15$  and  $1.19$  respectively compared to the  $1.8$  and  $1.7$  in Figures 3 and 4 respectively. In theory when  $M_{LB}=M_{SL}=M_{CR}$  then a beam is considered to be stable against lateral buckling.

*Moments capacities*

Tables 3 summarise the statistical properties for moments capacities applicable to Load case 1 and Load cases 2 and 3 respectively.

As commented previously, the measured moment capacities for Load cases 2 and 3 were merged as a consequence of the unexpected outcomes associated with beam tests in Load case 2.

**Table 3: Summary moment capacities**

Statistical Property	Moment capacities			
	Load case 1		Load cases 2 & 3	
	Lateral buckling limit state moment $M_{LB}$ <i>kNm</i>	Critical elastic lateral buckling moment, $M_{CR}$ <i>kNm</i>	Strength limit state moment $M_{SL}$ <i>kNm</i>	Critical elastic lateral buckling moment, $M_{CR}$ <i>kNm</i>
N	20	20	20	20
$X_{min}$	20.34	12.97	25.80	25.22
$X_{max}$	25.86	15.59	41.30	30.32
$X_{average}$	23.63	14.40	34.50	28.01
$X_{CoV}$	6.27%	4.83%	11.62%	4.8%
$X_{05}$	20.80	13.26	27.9	25.78
$X_{05,75}$	<b>20.77</b>	<b>13.06</b>	<b>26.76</b>	<b>25.39</b>

The values critical elastic buckling moment  $M_{CR}$  listed Table 3 and in Figures 4, 5, 6 and 7 were computed from the following Euler equation given in AS1720.1 from the measured values of  $EI_y$  and  $GJ$  for the beams tested.

$$M_{CR} = \left( \frac{\pi}{L_{ay}} \right) [EI_y GJ]^{1/2}$$

The values of  $M_{CR}$  listed in Table3 and in Figures 4, 5 6 and 7 were derived for  $L_{ay}=1,800\text{ mm}$  for Load case 2.

The values of  $M_{CR}$  are computed values being a function of the rigidities  $EI_y$  and  $GJ$ , whereas, the values the moment capacities for  $M_{LB}$  and  $M_{SL}$  are measured values derived from

$P(L-L_S)/4$  were  $P$  is the load measured during the tests. Hence, the low coefficient of variation of 4.83% for  $M_{CR}$  reflects the low coefficient of variations for the measured values of  $EI_y$  and  $GJ$  listed in Table 2.

It can be observed for Load cases 2 and 3 that the coefficient of variation for  $M_{SL}$  is 11.62%, this a very low value compared to sawn graded timber. On the other hand for Load case 1 the coefficient of variation for  $M_{LB}$  is 6.27% , this value is approximately half the value for  $M_{SL}$  in Load cases 2 and 3.. The lower coefficient of variation of  $M_{LB}$  reflects that this moment capacity is a function of the rigidities  $EI_y$  and  $GJ$  which have low coefficients of variations as listed in Table 2, whereas, the coefficient of variation of  $M_{SL}$  is a function of bending strength of the beams corresponding to the imposed moment at the instance of fracturing. All beams fractured within the load span, that is, within the zone of uniform moment.

For Load case 1, it can be observed for the statistic  $X_{05,75}$ , that  $M_{LB} > M_{CR}$  i.e. the ratio  $M_{LB} / M_{CR} = 1.60$ , hence the reason why these beams buckled. However, for Load cases 2 and 3  $M_{LB} \cong M_{CR}$  i.e. the ratio  $M_{LB} / M_{CR} = 1.05$ , these beams were for all intent and purpose stable. Applying the manufacturers values of  $EI_y$  and  $GJ$  for  $L_{ay} = 1,800 \text{ mm}$  gives a calculated value for  $M_{CR} = 19 \text{ kNm}$  compared to the value of  $M_{CR} = 25.39 \text{ kNm}$  derived from the measured values of  $EI_y$  and  $GJ$ , this is an increase of 34%. This increase in  $M_{CR}$  explains why buckling did not occur, as was initially expected for Load case 2 with  $L_{ay} = 1,800 \text{ mm}$ .

*Displacements and rotations*

Table 4 summarises the displacements and rotations measured during the testing.

The relationship between beam vertical displacement  $\Delta_x$ , lateral displacement  $\Delta_y$  and rotation  $\phi$  at mid-span is illustrated in Figure 7.

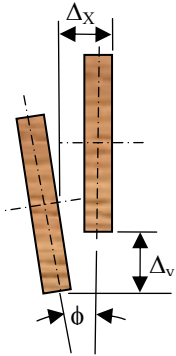


**Figure 7 : Measurement of displacements and rotation at mid-span**

For Load cases 2 & 3 only the vertical displacement is listed because the beams that fractured at  $L_{ay} = 1,800$  were not affected by lateral displacement similar to those beams when the mid-span restraint was fixed to reduce  $L_{ay}$  to 900 mm in Load case 3.

Table 4: Summary displacements and rotations

Statistical Property	Displacements and rotation						
	Load case 1					Load case 2 & 3	
	Mid span vertical displacement $\Delta_y @ M_{LB}$		Mid span lateral displacement $\Delta_x @ M_{LB}$		Average rotation $\phi @ M_{LB}$	Mid span vertical displacement $\Delta_y @ M_{SL}$	
	mm	$\Delta_y / L$	mm	$\Delta_x / L_{LS}$	degrees	mm	$\Delta_y / L$
N	20	20	20	20	20	20	20
$X_{min}$	55.67	0.010	8.04	0.002	1.55	66.01	0.012
$X_{max}$	66.11	0.012	38.79	0.011	5.97	87.56	0.016
$X_{average}$	62.68	0.012	20.80	0.006	3.60	78.17	0.014
$X_{CoV}$	4.25%	4.25%	45.65%	45.65%	39.52%	7.35%	7.35%
$X_{05}$	58.47	0.01	8.50	0.002	1.67	68.7	0.013
$X_{05,75}$	57.53	0.01	2.45	0.001	0.85	67.06	0.012

### Lateral Stability effect

In AS1720.1 the lateral stability effect is expressed by stability factor  $k_{12}$ . From AS 1720.1 the criteria for determining  $k_{12}$  is given as,

(a) For  $\rho S_1 \leq 10$ —

$$k_{12} = 1.0$$

(b) For  $10 \leq \rho S_1 \leq 20$ —

$$k_{12} = 1.5 - 0.5\rho S_1$$

(c) For  $\rho S_1 \geq 20$ —

$$k_{12} = \frac{200}{(\rho S_1)^2}$$

where,

$\rho$  = the material constant

$S_1$  = stability coefficient

In AS 1720.1 the material constant  $\rho$  for test purposes is calculated from the equation,

$$\rho = 14.71 \left( \frac{E}{f'_b} \right)^{-0.480}$$

Applying this equation to the test data gave  $\rho = 0.99$ ; this value corresponded with the manufacturers published value of  $\rho$ .

From AS1720.1 the stability coefficient  $S_1$  is given by the equation,

$$S_1 = \left[ \frac{1.1(EI)_x}{M_{cr} y_{max}} \right]^{1/2}$$

Substituting the equation for  $M_{CR}$  into the equation for  $S_1$  gives,

$$S_1 = \sqrt{\frac{2.2(EI)_x L_{ay}}{\pi d [(EI)_y (GJ)]^{1/2}}}$$

Applying this equation,  $\rho = 0.99$  and the criteria for  $k_{12}$ , values of  $k_{12}$  versus  $L_{ay}$  were computed for  $EI_x$ ,  $EI_y$  and  $GJ$  corresponding to the manufacturers calculated values and the measured values derived from the test data. The values of  $k_{12}$  applicable to the manufacturers calculated values and the measured test values are represented by Curve 1 and Curve 2 in Figure 8.

Compared to  $k_{12}$  calculated from AS1720.1, the lateral stability effect at the *lateral buckling limit states moment*  $M_{LB}$  for the beams tested can be expressed by the ratio of statistic  $X_{05,75}$ , corresponding  $M_{LB}$  and  $M_{SL}$ , that is, the ratio  $M_{05,75, LB}/M_{05,75, SL}$ . The ratio  $M_{05,75, LB}/M_{05,75, SL}$  is represented by Curve 3 in Figure 8, this curve is inferred from the measured bending capacities of the beams tested.

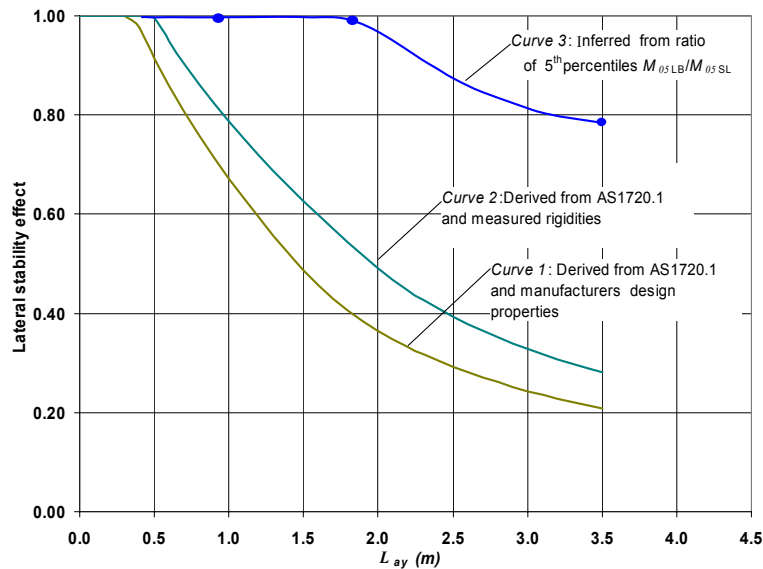


Figure 8: Lateral stability vs lateral restraint  $L_{ay}$

The difference between Curves 1 and Curve 2 reflects the difference in  $EI_x$ ,  $EI_y$  and  $GJ$  values calculated from the manufacturer's values and those measured from the test data. Curve 2 is that predicted by AS1720.1 whereas Curve 3 is that inferred from measured tests. Therefore, the difference between Curve 2 and Curve 3 is an indication of the degree of implicit conservatism in the rules of AS1720.1 for predicting the effects of beam slenderness on lateral buckling.

### Conclusion.

For slenderness ratios greater than 10, the design method in AS 1720.1 significantly underestimates moment capacity. The underestimation is partly attributable to the actual weak axis bending rigidities and torsional rigidities of the test pieces being greater than the nominal design values but nevertheless considerable scope exists to refine design procedures for LVL beams to optimise material use.

The objective to conduct a series of tests on LVL beams to observe their buckling behaviour and compare the behaviour with that predicted by the design rules of AS 1720.1 has been achieved.

### References:

1. Australian Standard AS 1720.1- 1997 Timber Structures Part 1: Design Methods.

2. AS/NZS 4357.0: Structural Laminated Veneer Lumber - Specifications
3. AS/NZS 4357.2: Structural Laminated Veneer Lumber – Determination of structural properties – Test methods
4. AS/NZS 4357.3: Structural Laminated Veneer Lumber – Determination of structural properties – Evaluation methods

## APPENDIX.

Photographs taken during LVL beam and torsion testing operations.

Load case 1 ( $L_{av}=1,800$  mm).



Load case 2 ( $L_{av}=1,800$  mm).



Load case 3 ( $L_{av}= 900$  mm)



Typical failure (Load case 2)



Torsion tests



